Journal of the Serbian Society for Computational Mechanics / Vol. 15 / No. 1, 2021 / pp 65-80
(10.24874/jsscm.2021.15.01.05)

FORCED CONVECTION IN A LID-DRIVEN NON-NEWTONIAN BLOOD FLOW THROUGH A STENOTIC ARTERY

Ignatius Fernandes[1*], Nitin Bodke[2]

[1] Government College, Quepem, Goa, India
e-mail: ignatius4u@gmail.com
[2] SSGG Commerce and Science College, Lonavala, India
e-mail: bodke.nitin@gmail.com
* *corresponding author*

Abstract

Cardiovascular diseases are one of the major health concerns globally, mainly caused by inadequate blood flow in different body parts. The lack of blood flow is often due to abnormal narrowing of blood vessels, and a systematic technique to boost blood flow in these areas can help cure the disease. One such method uses elevated temperatures to influence blood flow in the concerned areas. This paper investigates this process, i.e. the forced convection, through blood flow in a stenotic region of a human artery. A part of the stenotic region is considered a porous medium and the top wall is subjected to a higher temperature with a lid moving from left to right. Blood is considered as a non-Newtonian fluid with the power law index varying from 0.5 to 1.5. The geometric properties are considered to match the problem of blood flow in the artery affected by stenosis. The Carreau-Yasuda model is used to represent the non-Newtonian fluid flow in porous media and the numerical analysis is carried out using the Lattice Boltzmann method. This problem is investigated to study the influence of the moving lid and other geometric properties on convection and flow properties such as velocity profiles, streamlines, isotherms and heat transfer.

Keywords: Forced convection, blood flow, non-Newtonian fluids, Lattice Boltzmann method, lid.

1. Introduction

The mechanism of using elevated temperatures is a well-established tool to influence flow properties of fluid in fields such as biomedical research and groundwater flow. For instance, blood can be induced to higher temperatures to force its flow through infected areas in the human body to transport medicinal particles to a desired part of the body as in the case of aneurysm, thrombosis or stenosis. A good mathematical research in these areas does not only help to acquire a theoretical understanding of these problems, but it also provides a low-cost tool to investigate these processes. Most of the materials in this context exhibit porous medium like properties, thus a systematic study of forced convection in porous media has a very important role in modeling and analyzing these processes for future planning. However, the investigation of such a problem requires an understanding of many concepts such as forced convection, flow through porous

media, non-Newtonian fluids, blood flow and appropriate numerical techniques such as the Lattice Boltzmann method, which collectively help in addressing the problem. A brief chronological progress in these fields that is relevant for this study is provided below.

Forced convection in porous media, in its own way, has been investigated widely over many decades by a number of researchers. Shenoy (1994) provided a good review of non-Newtonian fluid heat transfer in porous media, also investigating the Darcy natural convection boundary layer problem. Afifi and Berbish (1999) presented results on forced convection over a horizontal plate in porous media. Pearson and Tardy (2010) presented a detailed insight into various models for transport in porous media. Sochi Taha (2010) carried out a study on four approaches used to describe flow in porous media: continuum models, capillary bundle models, numerical models and pore scale network models. Mehrizi et al. (2012) studied forced convection heat transfer in a square cavity with inlet and outlet slots and hot obstacle with and without a porous medium. These papers provide the basic understanding of flow in porous media required in this paper. Investigating fluid flow in porous media also depends on the right choice of the numerical tool in modeling and analyzing; and the Lattice Boltzmann method (LBM) has evolved as an efficient tool in simulating fluid flow in porous media. An overview of LBM and its efficiency in computing flow in a single and multi-phase fluid is can be found in Chen and Doolen (1998). Peng et al. (2004) proposed a simplified thermal LBM for incompressible thermal flow that is used in this paper. Seta et al. (2006) applied LBM to simulate forced convection in porous media using the Brinkman-Forchheimer equation. Mohamad (2011) also presented the working of LBM in simulating fluid flow, which can be used to study various phenomena such as natural and forced convection.

Simulation of blood flow can provide an effective aid in curing cardiovascular diseases such as aneurysm and stenosis. The formation of stenosis in arteries results in narrowing the blood flow path. Thus, understanding the flow properties in these processes is important to decide the medicinal process. This paper further uses these studies in investigating forced convection in a stenotic artery of the human body. Rheology of blood is discussed in detail by Merill (1969). Hu et al. (2015) used the Lattice Boltzmann method and smoothed profile method is proposed to simulate the forced and natural convection flows in complex geometries. Thomas and Sumam (2016) presented a review of the existing scenario of the simulation studies of blood flow, starting with a brief overview of the structure and function of arteries and veins. Ismael (2019) investigated the fluid-structure interaction (FSI) and forced convective heat transfer in a channel partly heated by constant heat flux and showed, using finite element method, that the compliant wall segment lowers the thermal performance of the non-baffled channel. Kim (2020) analyzed the fully developed laminar flow of the Cross fluid between parallel plates under uniform heat flux and derived the formulation of Nusselt number based on the analytically described velocity and flow rate. Maurya et al. (2019) investigated flow and thermal characteristics of the laminar forced convection of power-law fluids in a rectangular branching channel.

Various models have been proposed to represent blood flow out of which the Casson model has been widely used by many researchers. However, the disadvantage of this model is the limited validity of shear rate range, which is overcome by the Carreau Yasuda model. A large number of research studies considers blood to be Newtonian, though at low shear rates it is known to exhibit a non-Newtonian behavior. This paper investigates the influence of elevated temperatures on blood flowing through a stenotic region and on various flow properties such as velocity, temperature profiles and heat transfer. The results can help in providing a quantitative understanding of the influence of temperature in the treatment of cardiovascular diseases such as stenosis and aneurysm.

2. Problem description

Blood flows through a square stenotic geometry containing porous media with the top lid moving at a normalized temperature $T = 1$ and all other walls adiabatic. Blood enters the geometry with a uniform velocity U through the left wall along the horizontal direction. Darcy number Da and porosity ε are varied between 10^{-5} to 10^{-3} and 0.1 to 0.7, respectively, to match the geometrical properties of the stenotic artery, while Prandl number Pr is taken as 7. The relaxation parameter τ is varied locally based on the velocity of blood.

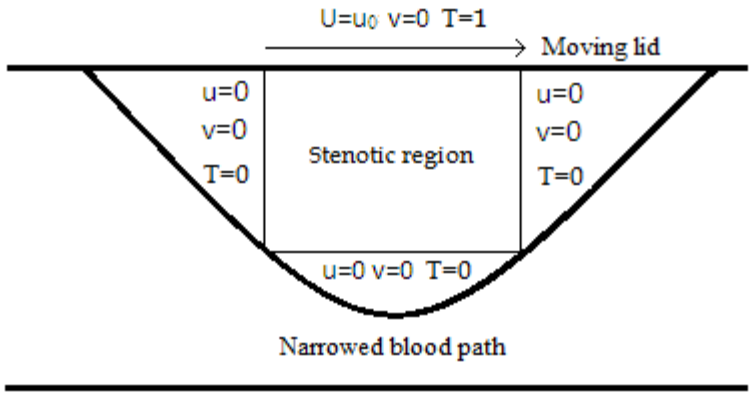

Fig. 1. Geometric representation of the problem.

The Carreau-Yasuda model is used to represent a non-Newtonian blood flow given by (Boyd et al. 2007)

$$\mu = \mu_0 + \left(\mu_0 - \mu_\infty\right) \Big/ \left(1 + a\left(\dot{\gamma}\right)^b\right)^{\frac{n-1}{b}} \tag{1}$$

where μ is the viscosity of the fluid, μ_0 and μ_∞ are viscosities at zero and infinite shear rate, respectively. The parameters a and b along with μ_0 and μ_∞ should be appropriately defined for the numerical simulation to converge, which depend on index n and material properties of the porous media.

3. Numerical method and boundary conditions

3.1 Governing Equations

The generalized model for incompressible flow in porous media is given by Peng et al. (2004)

$$\nabla . u = 0 \tag{2}$$

$$\frac{\partial u}{\partial t} + \left(u.\nabla\right)\left(\frac{u}{\varepsilon}\right) = -\frac{1}{\rho}\nabla\left(\varepsilon p\right) + v_e \nabla^2 u + F \tag{3}$$

where ρ is the fluid density, u and p are the volume-averaged velocity and pressure, respectively, and ε is the porosity of the porous medium. F is the total body force given by:

$$F = -\frac{\varepsilon\nu}{K}u - \frac{\varepsilon F_\varepsilon}{\sqrt{K}}|u|u + \varepsilon G \tag{4}$$

where v is the shear viscosity of the fluid and G is the body force. Permeability K and the Forcheimer's term F_ε are related to porosity ε (eps) as described by Ergun (1952)

$$F_\varepsilon = \frac{1.75}{\sqrt{150\varepsilon^3}}, \quad K = \frac{\varepsilon^3 d_p^2}{150(1-\varepsilon)^2} \tag{5}$$

where d_p is the solid particle diameter.

3.2 Lattice Boltzmann Method

For incompressible fluid flows and a nine-velocity model on a two-dimensional lattice (D2Q9), the LBM model is given by Guo and Zhao (2002)

$$f_i(x + e_i dt, t + dt) - f_i(x,t) = \frac{f_i^{eq}(x,t) - f_i(x,t)}{\tau} + dtF_i \tag{6}$$

where dt is increment in time, τ is the relaxation time, $f_i(x,t)$ represents the proportion of particles at time t positioned at x moving with a velocity e_i and $f_i^{eq}(x,t)$ is the equilibrium distribution function for D2Q9 given by

$$f_i^{eq}(x,t) = w_i\rho(x,t)\left[1 + \frac{1}{c_s^2}(e_i.u(x,t)) + \frac{1}{2\varepsilon c_s^4}(e_i.u(x,t))^2 - \frac{u(x,t)^2}{2\varepsilon c_s^2}\right] \tag{7}$$

The force term F_i is given by

$$F_i = w_i\rho\left(1 - \frac{1}{2\tau}\right)\left[\frac{e_i.F}{c_s^2} + \frac{uF:(e_i e_i - c_s^2 I)}{\varepsilon c_s^4}\right] \tag{8}$$

The fluid velocity u is given by

$$u = \frac{u_t}{c_0 + \sqrt{c_0^2 + c_1|u_t|}} \tag{9}$$

where u_t is a temporal velocity given by

$$u_t = \sum_i e_i f_i + \frac{dt}{2}\rho\varepsilon G \tag{10}$$

The two parameters in Eq. 9 are given by

$$c_0 = \frac{1}{2}\left(1 + \varepsilon\frac{dt}{2}\frac{v}{K}\right), \quad c_1 = \varepsilon\frac{dt}{2}\frac{F_E}{\sqrt{K}} \tag{11}$$

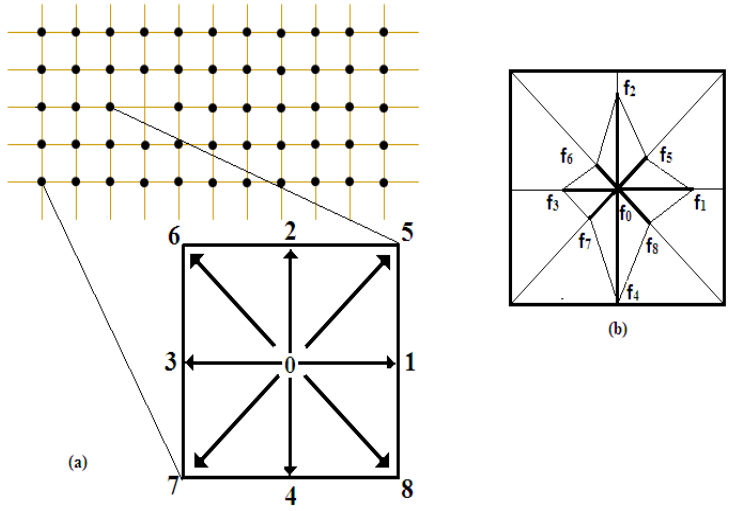

Fig. 2. (a) Amplified position of a D2Q9 lattice model; (b) Distribution functions.

A D2Q9 lattice model is a two-dimensional nine-node lattice model as shown in Figure 2, which is the most frequently used model used in simulating fluid flow in porous media.

3.3 Energy Equation

The thermal lattice Bhatnagar-Gross-Krook (BGK) model proposed by Peng (2004) is used to model heat transfer

$$g_i(x + e_i dt, t + dt) - g_i(x,t) = \frac{g_i^{eq}(x,t) - g_i(x,t)}{\tau_g} \tag{12}$$

$g_i(x,t)$ is the thermal distribution function, τ_g the relaxation time and $g_i^{eq}(x,t)$ is the equilibrium distribution function given by (Mehrizi et al., 2013)

$$g_0^{eq}(x,t) = -\frac{2\rho\varepsilon}{3}\frac{u^2}{c_s^2} \tag{13}$$

$$g_i^{eq}(x,t) = \frac{\rho\varepsilon}{9}\left[\frac{3}{2} + \frac{3}{2}\frac{e_i.u}{c_s^2} + \frac{9}{2}\frac{(e_i.u)^2}{c_s^4} - \frac{3}{2}\frac{u^2}{c_s^2}\right] (i = 1,2,3,4) \tag{14}$$

$$g_i^{eq}(x,t) = \frac{\rho\varepsilon}{36}\left[3 + \frac{6}{2}\frac{e_i.u}{c_s^2} + \frac{9}{2}\frac{(e_i.u)^2}{c_s^4} - \frac{3}{2}\frac{u^2}{c_s^2}\right] (i = 5,6,7,8) \tag{15}$$

Reynolds number, $\mathrm{Re} = \frac{UL}{\upsilon}$, where U and L are the characteristic velocity and the characteristic length, respectively.

3.4 Boundary Conditions

Second order bounce back rule for non-equilibrium distribution function f_i are used to determine velocity on the four walls. The distribution functions are given by (Zuo and He 1997; Seta et al. 2006)

$$f_{\alpha}^{neq} = f_{\beta}^{neq} \tag{16}$$

where β is the opposite direction of α.

At the lattice nodes on the moving walls, boundary conditions are assumed as specified by Zou et al. (Zuo and He, 1997) given by

$$f_4 = \frac{1}{9\rho}\left[1-3v+\frac{9}{2}v^2-\frac{3}{2}\left(u^2+v^2\right)\right] \tag{17}$$

$$f_7 = \frac{1}{36\rho}\left[1-3\left(-u-v\right)+\frac{9}{2}\left(u+v\right)^2-\frac{3}{2}\left(u^2+v^2\right)\right] \tag{18}$$

$$f_8 = \frac{1}{36\rho}\left[1+3\left(u-v\right)+\frac{9}{2}\left(u-v\right)^2-\frac{3}{2}\left(u^2+v^2\right)\right] \tag{19}$$

For energy distribution function g_i, second order extrapolation rule is used on the right wall and the boundary conditions for all other walls were defined as per method introduced by D'Orazio et al. (2004). The distribution functions on the left wall were defined as

$$g_1 = \frac{6}{9}\left(1-T_p\right),\ g_5 = \frac{1}{36}T^{eq}\left(1+3(u+v)\right),\ \ g_8 = \frac{1}{36}T^{eq}\left(1+3(u-v)\right) \tag{20}$$

where

$$T_p = g_0 + g_2 + g_3 + g_4 + g_6 + g_7$$

and

$$T^{eq} = \frac{-6T_p}{1+3u} \tag{21}$$

The distribution functions on the top wall were defined as

$$g_4 = \frac{1}{9}T^{eq}(1+3u),\ \ g_7 = \frac{1}{36}T^{eq}\left(1+3(u+v)\right),\ \ g_8 = \frac{1}{36}T^{eq}\left(1+3(u-v)\right) \tag{22}$$

where

$$T_p = g_0 + g_1 + g_2 + g_3 + g_5 + g_6$$

and

$$T^{eq} = \frac{6\left(1-T_p\right)}{1+3u} \tag{23}$$

The distribution functions on the bottom wall were defined as

$$g_2 = \frac{1}{9}T^{eq}(1+3u), \quad g_5 = \frac{1}{36}T^{eq}\left(1+3(u+v)\right), \quad g_6 = \frac{1}{36}T^{eq}\left(1+3(u-v)\right) \tag{24}$$

where

$$T_p = g_0 + g_1 + g_3 + g_4 + g_7 + g_9$$

and

$$T^{eq} = \frac{-6T_p}{1+3u} \tag{25}$$

4. Results and Discussion

For non-Newtonian fluids, Darcy's law for fluid flowing through a porous media is given by

$$q = \left(\frac{K}{\mu_{eff}}\frac{\nabla p}{L}\right)^{1/n} \tag{26}$$

where q is Darcy flux, μ_{eff} is the effective viscosity, ∇p is the pressure gradient and L is the characteristic length. Thus, validity of the numerical procedure for non-Newtonian numerical simulation can be established by verifying that the plot of q and $\nabla p = grad(p)$ is linear with slope $1/n$ as given in Table 1. The convergence of numerical simulation depends on how appropriately the parameters involved in Eq.1 are selected. The relaxation parameter depends on the local strain that is given by (Leonardi et al. 2011)

$$\gamma_{\alpha\beta} = \frac{-3}{2\rho c^2 \tau dt}\sum_i e_{i\alpha}e_{i\beta}\left(f_i - f_i^{eq}\right) \tag{27}$$

n	Da	ε		
		0.1	0.4	0.7
0.5	10^{-5}	1.9822	1.9654	1.9673
	10^{-3}	1.9605	1.9666	1.9794
	10^{-1}	2.0584	2.0267	2.0644
1	10^{-5}	1.0166	1.0208	1.0132
	10^{-3}	0.9857	1.0343	1.0196
	10^{-1}	1.0483	0.9807	1.0325
1.5	10^{-5}	0.7254	0.7188	0.6908
	10^{-3}	0.6898	0.6801	0.7015
	10^{-1}	0.7144	0.7039	0.7183

Table 1. Slope values for plot of q versus ∇p.

Parameters μ_0 and μ_∞ determine the range of values for τ; range of which is very small and important for the convergence criteria. The values of the parameters μ_0 and μ_∞ are set in the range

of 0.001 and 0.2. Parameter a and b in Eq. 1 are set in the range 0.001 to 0.1 and 0.5 to 10, respectively, depending the value of n and Da.

Figure 3 shows the variation in u-velocity profiles (horizontal component) for Re=10 and $\varepsilon = 0.1$ based on the variation in n. The influence of the moving lid is seen on the velocity, as the profiles are smooth curves at the left corner whereas the velocity drops on the other end. Though the basic trend of the velocity profiles remains the same as n varies from 0.5 to 1.5, the difference is in terms of the magnitude; and the shear-thickening fluids ($n = 1.5$) show higher velocities compared to the shear-thinning fluids ($n = 0.5$). Since blood behaves more like a shear-thinning fluid, its velocities are expected to be in the range corresponding to the values of n from 0.5 to 1.0. The profile for $n = 1$ represents the Newtonian fluids. The inclined behavior of the velocity profiles is due to the movement of lid which is absent in case the lid is kept stationary, as seen in Fig. 4. The velocity in this case follows a symmetric behavior, while the magnitude of velocity for $n = 1.5$ is seen to be higher than the case where the lid is moving. That is because the lid and the fluid are moving in the same direction. However, for $n = 0.5$ and $n = 1$, the velocity of the moving lid was seen to be higher than in the case where the lid is stationary.

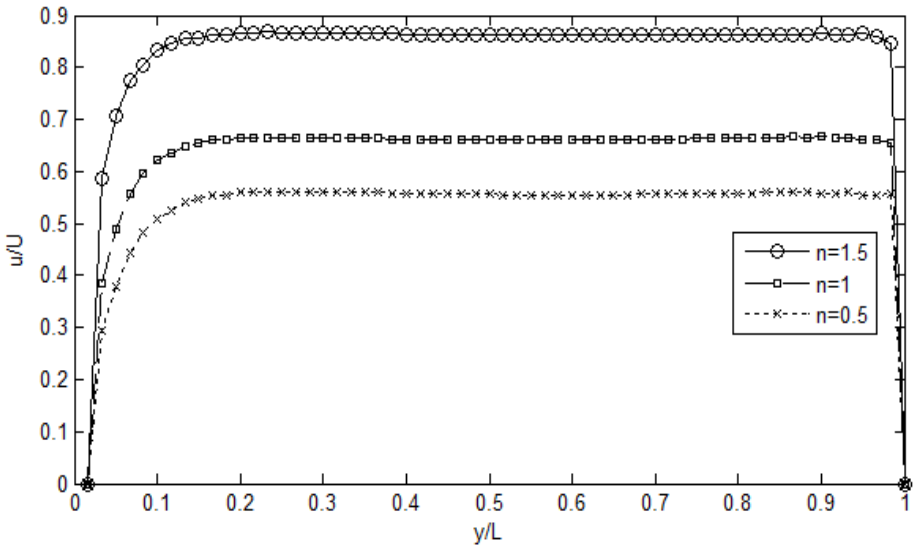

Fig. 3. Variation in u-velocity profiles for different values of n at Re=10 and $\varepsilon = 0.1$ with a moving lid.

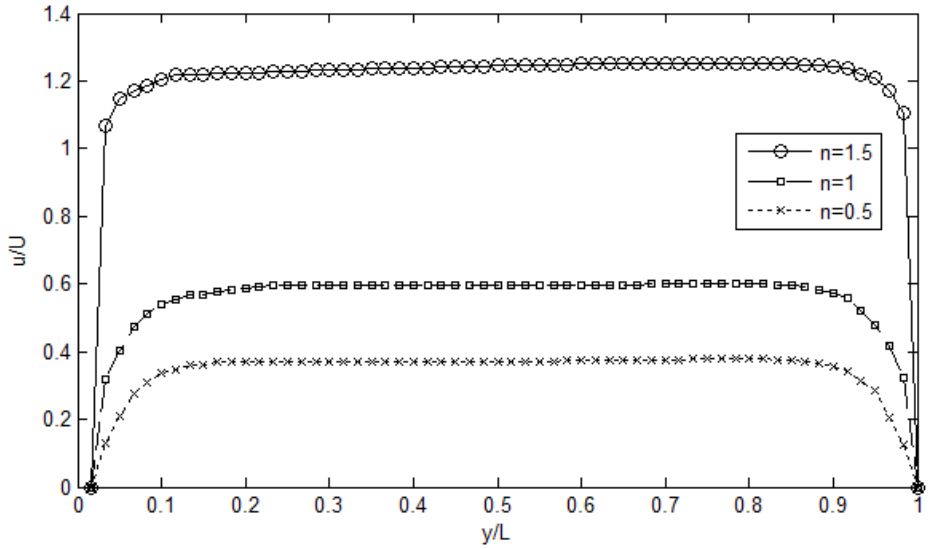

Fig. 4. Variation in u-velocity profiles for different values of n at Re=10 and $\varepsilon = 0.1$ with a stationary lid.

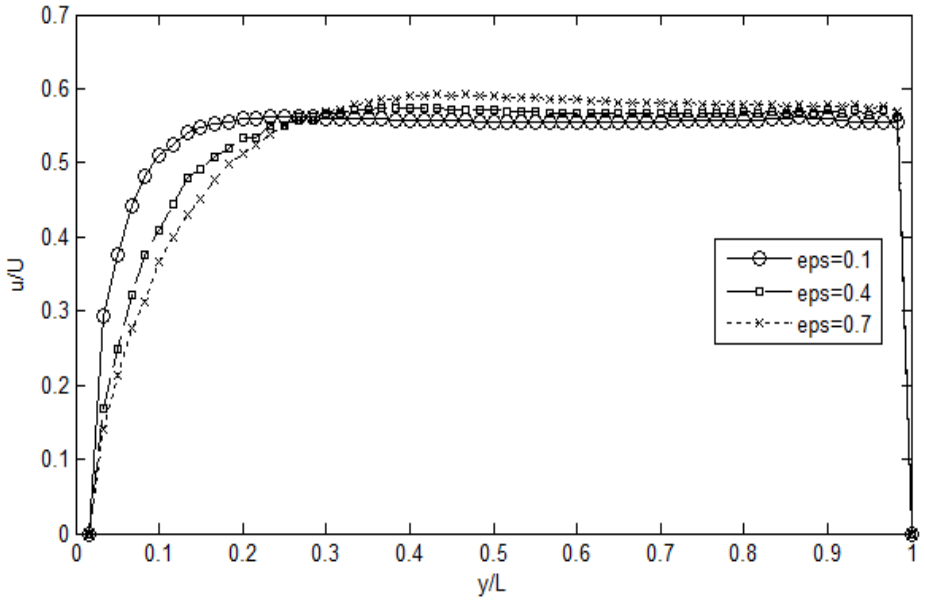

Fig. 5. Variation in u-velocity profiles for different values of ε at Re=10 and $n = 0.5$.

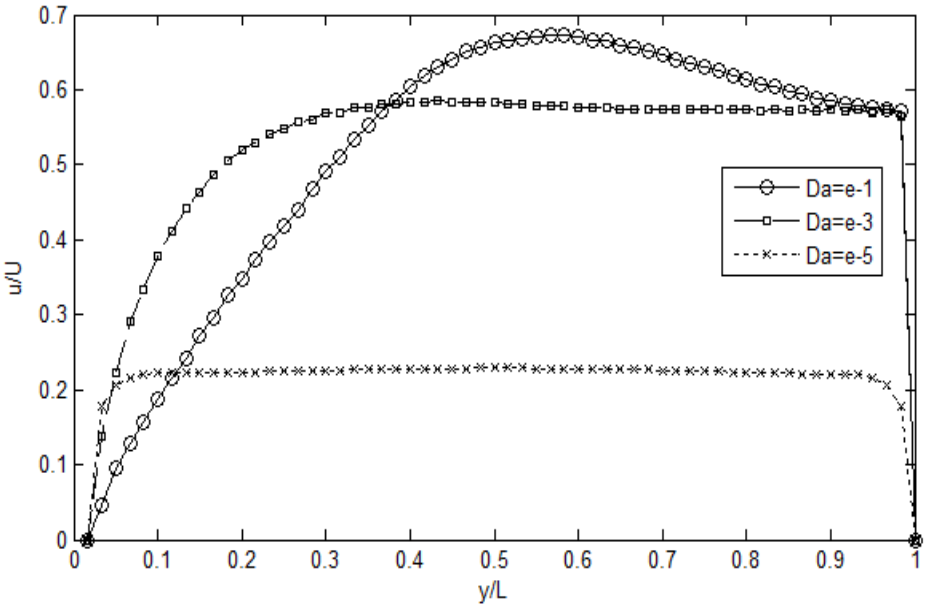

Fig. 6. Variation in u-velocity profiles for different values of Da at $n = 1.5$ and $\varepsilon = 0.4$.

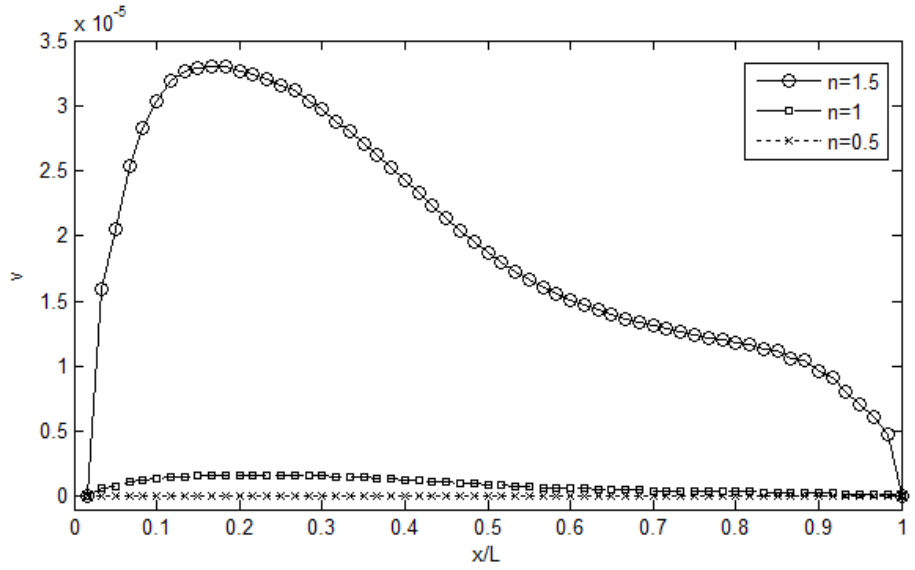

Fig. 7. Variation in v-velocity profiles for different values of n at Re=10 and $\varepsilon = 0.4$.

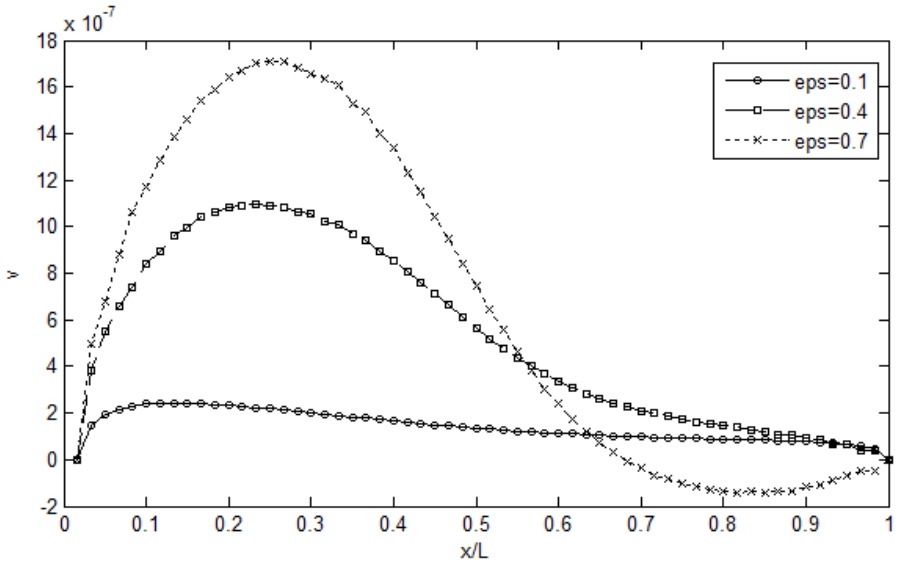

Fig. 8. Variation in v-velocity profiles for different values of ε at Re=10 and $n = 1.5$.

Figure 5 shows the variation in u-velocity based on the variation in ε from 0.1 to 0.7. Though not much difference is seen in the peak value, major difference is seen in the curve of the profiles with the curve getting steeper as ε increases from 0.1 to 0.7. Figure 6 shows the variation in fluid velocity based on the variation in Da from 10^{-5} to 10^{-1}. A much stronger influence of Da is observed on the velocity as the velocity profiles change both in magnitude and trend as Da increases from 10^{-5} to 10^{-1}.

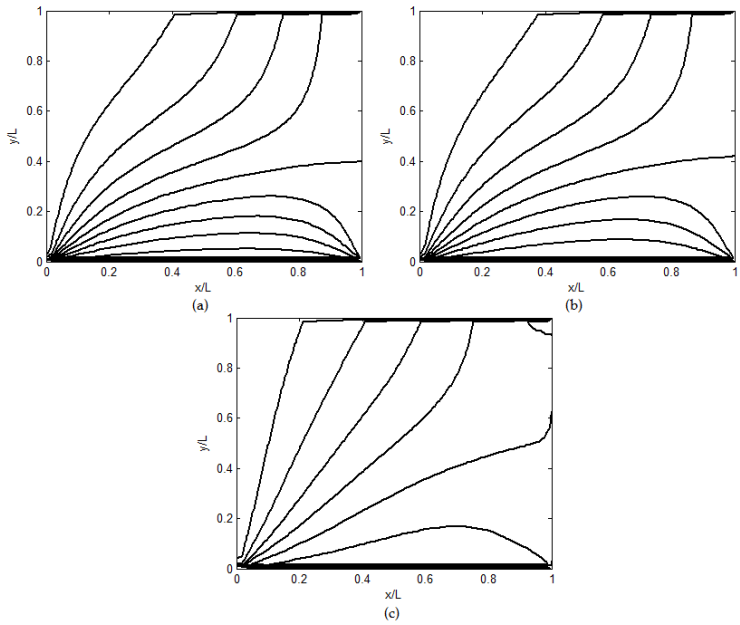

Fig. 9. Isotherms for $\varepsilon = 0.4$ and $n = 1$ at (a) Re=0.01 (b) Re=1 (c) Re=100.

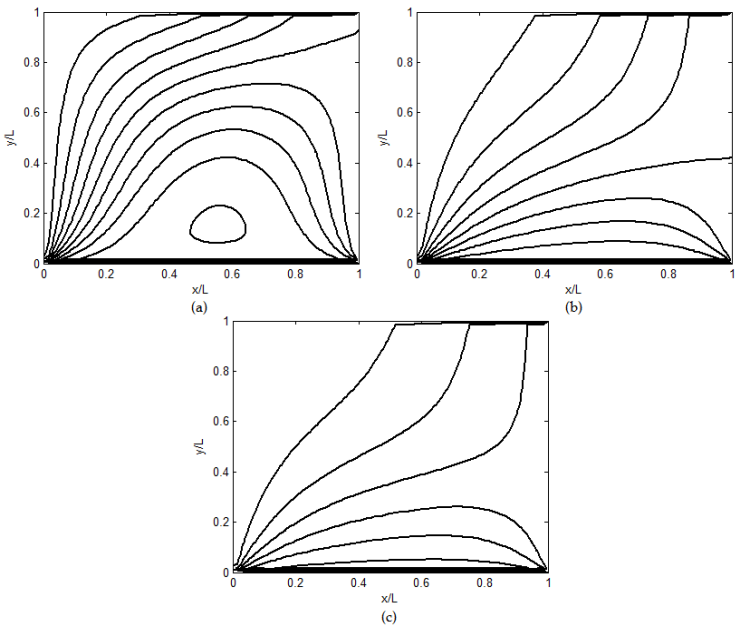

Fig. 10. Isotherms at $\varepsilon = 0.4$ and Re=10 at (a) n =0.5 (b) n =1 (c) n =1.5.

As Da increases, the influence of the lid also becomes stronger as the profiles are seen to be steeper for higher values of Da. The trend of velocity profiles for $Da = 10^{-5}$ are almost the same as in the case of stationary lid. While for power law index n the shape of the profiles does not change, in the case of Da the profiles show higher variations. The influence of Da, which also relates directly to the permeability of the region, and n is observed to be higher than the porosity. Variations in v-velocity profiles (vertical velocity) based on the variation in n and ε are presented in Fig. 7-8. As n increases, the v-velocity is seen to increase with higher velocities at the left side of the geometry. The movement of the lid from left to right tends to have lesser influence on the vertical component towards the right side of the geometry.

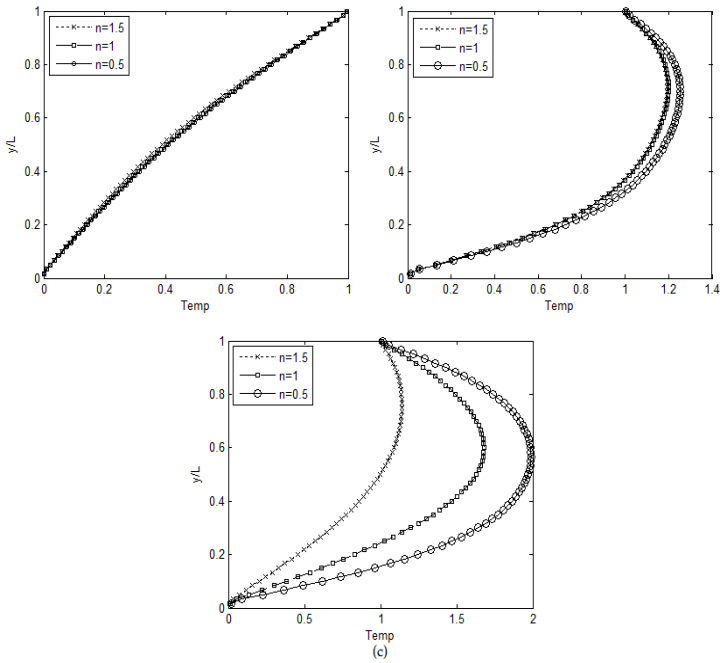

Fig. 11. Temperature profiles at three axial positions on horizontal axis for $\varepsilon = 0.4$, Re=10 and different values of n at (a) 1st quartile (b) 2nd quartile (c) 3rd quartile.

The variation increases uniformly with respect to porosity, which is not the case with respect to power law index, and the velocity jumps by higher margin for shear-thickening fluids. The formation of a vortex is seen for n =0.5, while also expanding the heat transfer to a bigger part of the geometry. A stronger heat transfer is observed in blood as compared to shear-thickening fluids, thus suggesting an effective tool to transfer energy through blood, as seen in Fig. 9-10. Power law index n and permeability K plays the most crucial role while using elevated temperatures on blood. In addition, the movement of the lid is also seen to be very effective in influencing the flow properties. Figure 11 shows the temperature profiles at three axial positions on the horizontal side of the geometry and its variation based on n. The influence of the moving lid and n is clearly seen on the temperature of the fluid at the three positions and a significant difference in the temperature is seen as n varies from 0.5 to 1.5. Shear thinning fluids show a stronger heat transfer as compared to shear-thickening fluids.

$\boldsymbol{n}$	$\boldsymbol{Da}$		
	10^{-5}	10^{-3}	10^{-1}
0.5	0.8588	0.9015	1.0406
1.0	1.1000	1.1000	1.1000
1.5	1.3917	1.5001	2.2996

Table 2. Average τ values for various values of n and Da.

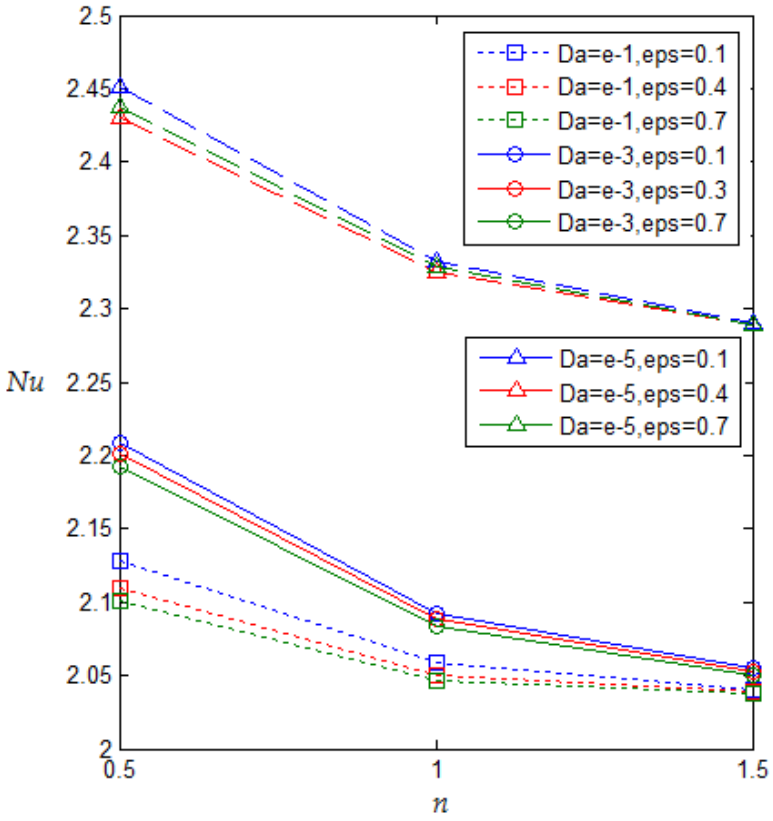

Fig. 12. Variation in Nu for various values of Da, ε and n.

The curve behavior is due to the moving lid, and the temperature is seen to be higher for $n = 0.5$ as compared to $n = 1$ and $n = 1.5$. The temperature is seen to be higher at the far end as compared to the left side of the geometry ascertaining the recommendation on the use of temperatures on blood to influence its properties. The relaxation parameter determines the effective viscosity at micro level and hence varies locally. Table 2 provides the average value τ based on the values of n and Da. Figure 12 shows the variation in Nusselt number based on the variations in Da, ε and n. The influence of Da is seen the highest on Nu while the least influence is seen of porosity. Nu decreases as n increases from 0.5 to 1.5. The drop in Nu for n varying from 0.5 to 1 is higher than the values from 1 to 1.5, indicating that the heat transfer can be stronger in blood as compared to shear-thickening fluids. Da also plays a very important role in Nu, as we can see from Fig. 12, and the variation of Da values from 10^{-5} to 10^{-3} is higher than that of 10^{-3} to 10^{-1}. Though Nu decreases as ε increases, the drop is not seen to be very significant as compared to the behavior with respect to Da and n. Blood flow has a very important role in transporting medicinal treatment to these affected areas. It is evident that the moving lid has a significant influence on the flow properties in the areas affected by stenosis. Among all the geometric properties, it is evident that permeability has the highest influence on the flow properties followed by the power law index.

5. Conclusion

The paper has investigated the influence of elevated temperatures on blood flow through a stenotic artery. Blood was considered a non-Newtonian fluid and the influence of physical properties such as power law index, porosity and permeability of the porous medium was studied on the flow parameters including velocity profiles, temperature profiles and heat transfer. The Darcy number and the power law index showed a higher influence on the flow properties as compared to porosity. A significant influence of a moving lid was also seen on velocity profiles as compared to a stationary lid suggesting that a horizontal motion of a hot lid over a surface results in a stronger heat transfer and other properties of transport phenomena. In addition, a much stronger influence of power law index was observed on heat transfer as shear-thinning fluids showed a stronger heat transfer as compared to shear-thickening fluids. Since blood behaves as a shear-thinning fluid, the results validated the use of elevated temperature in a systematic management of blood flow as required by the process under consideration. The results also showed the efficiency of the moving lid in obtaining better need-based results as compared to the stationary lid.

References

Afifi, R. I. And Berbish, N. S. (1999). Experimental investigation of forced convection heat transfer over a horizontal flat plate in a porous medium, J. Engg. Appl. Sci. 46, 693–710.

Boyd Joshua, Buick James M. (2007). Analysis of the Casson and Carreau-Yasuda non-Newtonian blood models in steady and oscillatory flows using the lattice Boltzmann method, Physics of Fluids 19, 093103.

Chen Shiyi, Doolen Gary D. (1998). Lattice Boltzmann method for fluid flows, Annu. Rev. Fluid Mech. 30, 329-364.

D'Orazio A., Corcione M., Celata G. P. (2004). Application to natural convection enclosed flows of a lattice Boltzmann BGK model coupled with a general purpose thermal boundary condition, Int. J. Therm. Sci. 43 (6), 575–586.

Ergun S. (1952), Flow Through Packed Columns, Chem. Eng. Process, vol. 48, 89–94.

Hu Yang, Li Decai, Shu Shi, Niu Xiaodong (2015). *An efficient smoothed profile-lattice Boltzmann method for the simulation of forced and natural convection flows in complex geometries*, International Communications in Heat and Mass Transfer, Volume 68, 188-199.

Ismael Muneer A. (2019). *Forced convection in partially compliant channel with two alternated baffles*, International Journal of Heat and Mass Transfer, Volume 142, 118455.

Kim Sun Kyoung, *Forced convection heat transfer for the fully-developed laminar flow of the cross fluid between parallel plates*, Journal of Non-Newtonian Fluid Mechanics, Volume 276(2020):104226.

Leonardi C.R., Owen D.R.J., Feng Y.T. (2011). Numerical Rheometry of Bulk Materials using a Power Law Fluid and the Lattice Boltzmann Method, J. Non-Newtonian Fluid Mech., vol. 166, 628–638.

Maurya Anamika, Tiwari Naveen, Chhabra R.P. (2019). *Effect of inclination angle on the forced convective flow of a power-law fluid in a 2-D planar branching channel*, International Journal of Heat and Mass Transfer, Volume 134, 768-783.

Mehrizi Abouei A, Farhadi M., Sedighi K., Delavar Aghajani M. (2013). Effect of fin position and porosity on heat transfer improvement in a plate porous media heat exchanger, Journal of the Taiwan Institute of Chemical Engineers, 44, 420–431.

Mehrizi Abouei A, Sedighi K., Afrouzi H Hassanzade, Aghili A. Latif (2012). Lattice Boltzmann simulation of forced convection in vented cavity filled by porous medium with obstruction, World Applied Sciences Journal 16, 31-36.

Merrill W. Edward (1969). Rheology of blood, Physiological Reviews, 40(4), 863-888.
Mohamad A. (2011). Lattice Boltzmann method, Springer- Verlag London Limited.
Pearon J. R. A., Tardy P. M. J. (2002). Models for flow of non-Newtonian and complex fluids through porous media, Journal of Non-Newtonian Fluid Mechanics 102, 447-473.
Peng Y, Shu C, Chew Y T. (2004). A 3D incompressible thermal lattice Boltzmann model and its application to simulate natural convection in a cubic cavity, J Comput Phys, 74, 193-260.
Seta T, Takegoshi E, Okui K. (2006). Lattice Boltzmann simulation of natural convection in porous media, Mathematics and Computers in Simulation 72, 195–200.
Seta T, Takegoshi E, Kitano K, Okui K. (2006). Thermal lattice Boltzmann model for incompressible flows through porous media, Journal of Therm Science and Technology 1(2), 90-100.
Shenoy A. V. (1994). Non-Newtonian Fluid Heat Transfer in Porous Media, Advances in Heat Transfer, Volume 24, 101-190.
Sochi Taha (2010). Non-Newtonian flow in porous media, Polymer 51, 5007-5023.
Sumam K. S., Thomas Blessy (2016). Blood Flow in Human Arterial System-A Review, Procedia Technology 24, 339-346.
Z. Guo, and T.S. Zhao (2002). Lattice Boltzmann Model for Incompressible Flows through Porous Media, Phys. Rev. E, vol. 66, p. 036304.
Zou Qisu, He Xiaoyi (1997). On pressure and velocity boundary conditions for the lattice Boltzmann BGK model, Phys. Fluid, 9(6).